Enzyme Catalysis Hot Paper

How to cite: *Angew. Chem. Int. Ed.* **2022**, *61*, e202211382
International Edition: doi.org/10.1002/anie.202211382
German Edition: doi.org/10.1002/ange.202211382

Discovery of a Unique Structural Motif in Lanthipeptide Synthetases for Substrate Binding and Interdomain Interactions

Shanqing Huang[+], Ying Wang[+], Chuangxu Cai, Xiuyun Xiao, Shulei Liu, Yeying Ma, Xiangqian Xie, Yong Liang, Hao Chen, Jiapeng Zhu, Julian D. Hegemann, Hongwei Yao,* Wanqing Wei,* and Huan Wang**

Abstract: Class III lanthipeptide synthetases catalyze the formation of lanthionine/methyllanthionine and labionin crosslinks. We present here the 2.40 Å resolution structure of the kinase domain of a class III lanthipeptide synthetase CurKC from the biosynthesis of curvopeptin. A unique structural subunit for leader binding, named leader recognition domain (LRD), was identified. The LRD of CurKC is responsible for the recognition of the leader peptide and for mediating interactions between the lyase and kinase domains. LRDs are highly conserved among the kinase domains of class III and class IV lanthipeptide synthetases. The discovery of LRDs provides insight into the substrate recognition and domain organization in multidomain lanthipeptide synthetases.

Introduction

Lanthipeptides belong to the superfamily of ribosomally synthesized and posttranslationally modified peptide (RiPP) natural products and typically contain the β-thioether crosslinked amino acids lanthionine (Lan) and methyllanthionine (MeLan).[1] The Lan/MeLan crosslinks are typically generated by the enzymatic dehydration of serine/threonine residues that yields dehydroalanine (Dha)/dehydrobutyrine (Dhb), respectively, and the subsequent cyclization between cysteine and Dha/Dhb catalyzed by designated cyclases. To date, five classes of lanthipeptides have been reported based on the characteristics of their biosynthetic enzymes.[1b,2] Class I lanthipeptides utilize a combination of aminoacyl-tRNA-dependent dehydratases (LanBs) and cyclases (LanCs),[3] whereas class II lanthipeptides are biosynthesized by ATP-dependent bifunctional lanthipeptide synthetases (LanMs).[4] The biosynthesis of class III and class IV lanthipeptides relies on a group of three-domain enzymes named LanKCs and LanLs, respectively, which contain an N-terminal lyase, a central kinase, and a C-terminal cyclase domain.[5] These three domains perform the sequential modification of the core peptides in the order of 1) NTP-dependent Ser/Thr phosphorylation, 2) phosphate elimination that yields Dha/Dhb and 3) Michael addition between Cys and Dha/Dhb to generate the thioether linkages (Figure 1). LanCs, LanMs, and LanLs utilize a zinc ion in their respective cyclase domains that acts as a Lewis acid for activating the Cys thiol during Lan/MeLan formation. In contrast, the cyclase domains of LanKCs do not contain a conserved Zn binding motif, indicating that LanKC-cata-

[*] Dr. S. Huang,[+] Y. Wang,[+] C. Cai, X. Xiao, Y. Ma, X. Xie, Prof. Dr. Y. Liang, Prof. Dr. H. Chen, Prof. Dr. H. Wang
State Key Laboratory of Coordination Chemistry, Chemistry and Biomedicine Innovation Center of Nanjing University, Jiangsu Key Laboratory of Advanced Organic Materials, School of Chemistry and Chemical Engineering,
Nanjing University
No. 163 Xianlin Ave, Nanjing, 210093 (China)
E-mail: wanghuan@nju.edu.cn

S. Liu, Prof. Dr. H. Yao
Institute of Molecular Enzymology, School of Biology and Basic Medical Sciences, Soochow University
Suzhou, 215123 (China)
E-mail: hwyao@suda.edu.cn

Dr. J. D. Hegemann
School of Medicine and Life Sciences, State Key Laboratory Cultivation Base for TCM Quality and Efficacy, Jiangsu Key Laboratory for Pharmacology and Safety Evaluation of Chinese Materia Medica, Nanjing University of Chinese Medicine
Nanjing 210023 (China)
E-mail: Julian.Hegemann@helmholtz-hips.de

Prof. Dr. J. Zhu
Helmholtz Institute for Pharmaceutical Research Saarland (HIPS), Helmholtz Centre for Infection Research (HZI), Saarland University Campus
66123 Saarbrücken (Germany)

Dr. W. Wei
State Key Laboratory of Food Science and Technology, Jiangnan University, Wuxi 214122 (P. R. China)
E-mail: wanqwei@163.com

[+] These authors contributed equally to this work.

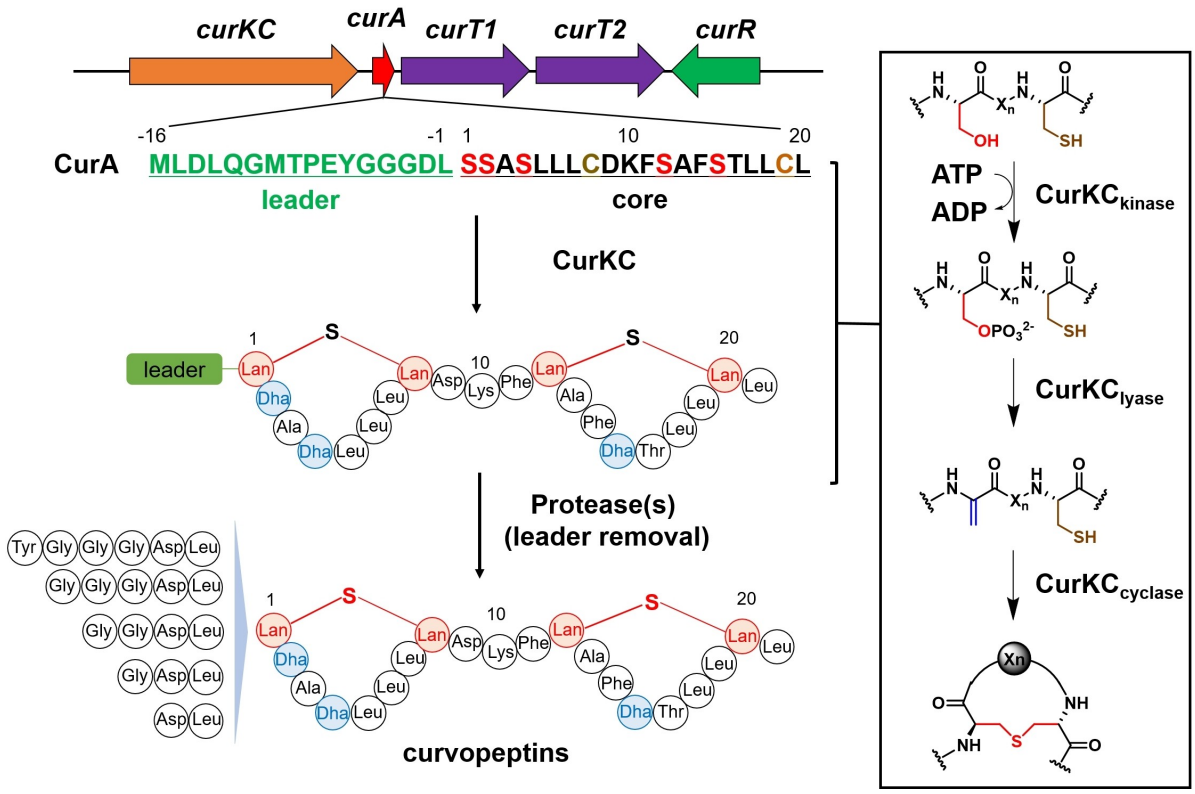

Figure 1. Biosynthesis of the class III lanthipeptide curvopeptin congeners. The biosynthetic gene cluster contains genes encoding the following proteins: a class III lanthipeptide synthase (CurKC), a precursor peptide (CurA), two ABC transporters (CurT1/T2) and a regulatory protein (CurR). The leader peptide is possibly removed by bifunctional M1 family aminopeptidase(s) encoded in the genome of the producing strain *Thermomonospora curvata* DSM43183.[9] Incomplete removal of the leader peptide by the aminopeptidase(s) leads to the production of congeners with leader overhangs of various lengths.

lyzed macrocyclization is Zn-independent.[6] In accordance with the distinct cyclase feature, LanKCs are the only lanthipeptide synthetases observed to catalyze the formation of tri-amino acid crosslinks, named labionin, through the sequential formation of a C–S and a C–C bond.[7] To date, mechanistic investigation of LanBs, LanCs and LanMs is supported by crystallography studies,[3a,b,4a] whereas crystal structures of LanKC/LanL enzymes or their individual domains remain unavailable. Herein, we report the first crystal structure of the kinase domain of CurKC, the class III lanthipeptide synthetase responsible for the biosynthesis of curvopeptin.[8] A unique leader recognition domain (LRD) was identified in the kinase domain of CurKC, which consists of two N-terminal antiparallel β-sheets, a central α-helix and three C-terminal antiparallel β-sheets. This LRD motif is highly conserved among class III and class IV lanthipeptide synthetases and is responsible for both the leader peptide binding and the interaction between their lyase and kinase domains.

Results and Discussion

CurKC displays a three-domain organization:an N-terminal lyase domain (residues 1–217, denoted as CurKC$_{lyase}$), a central kinase domain (residues 218–489, denoted as CurKC$_{kinase}$), and a C-terminal cyclase domain (residues 594–866, denoted as CurKC$_{cyclase}$) (Figure S1–S3). Heterologous expression of full-length CurKC, CurKC$_{lyase}$, CurKC$_{kinase}$, CurKC$_{lyase\text{-}kinase}$ (residues 1–489) and CurKC$_{kinase\text{-}cyclase}$ (residues 218–866) in *E. coli* BL21(DE3) all yielded soluble proteins (Figure S4). CurKC$_{cyclase}$, however, was not detected in soluble or insoluble fractions after expression in *E. coli* BL21(DE3), suggesting that CurKC$_{cyclase}$ is incapable of folding into a stable protein independently. A C-terminal truncated variant of the CurA peptide, named CurA$_S$, was employed as a substrate for enzymatic assays as it is significantly more accessible by chemical synthesis than the full length CurA (Figure 2). In the presence of ATP and Mg^{2+} ions, CurKC modified CurA$_S$ by one- and two-fold dehydration along with partial phosphorylation, as determined by matrix-assisted laser desorption time-of-flight mass spectrometry (MALDI-TOF MS) (Figure S5). The incomplete dehydration of CurA$_S$ by CurKC was in agreement with previous studies showing that the disruption of the C-terminal Lan formation impairs the modification of Ser/Thr residues at the N-terminal core peptide.[5b] CurKC$_{kinase}$ modified CurA$_S$ by one-fold phosphorylation, indicating that the kinase domain of CurKC can fold and function independently. Co-incubation of CurKC$_{lyase}$ and CurKC$_{kinase}$ with CurA$_S$ led to a similar result as the incubation of CurA$_s$ with CurKC$_{lyase\text{-}kinase}$: a single dehydra-

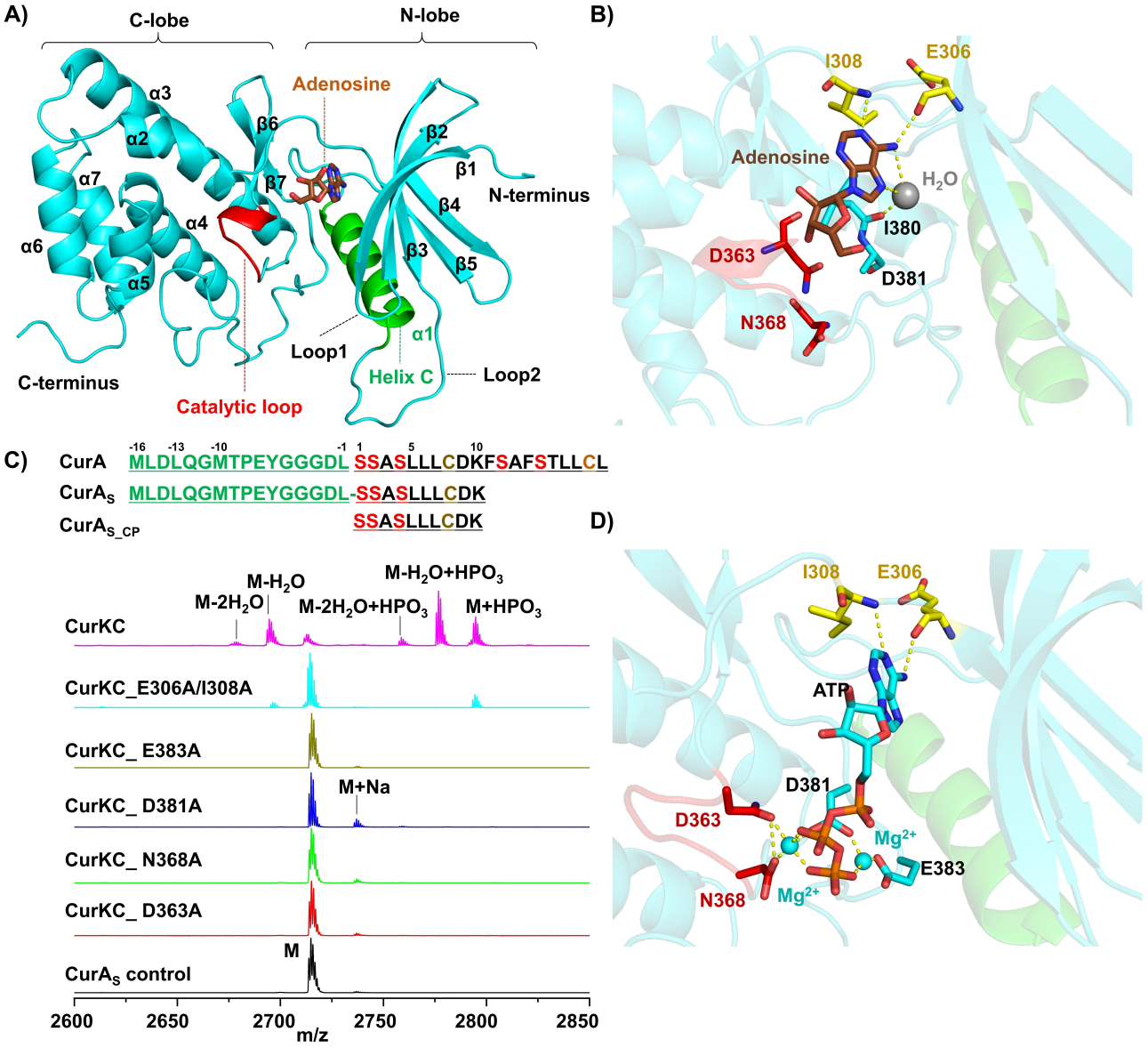

Figure 2. A) Crystal structure of the $CurKC_{kinase}$–adenosine complex. The adenosine molecule is shown in a stick representation. B) Close-up view of the adenosine binding site. Adenosine and interacting residues are shown as sticks, and the water molecule is shown as a gray sphere. Hydrogen bonds are shown as yellow dashed lines. Oxygen and nitrogen atoms are colored red and blue, respectively. C) MALDI-TOF MS analysis of the in vitro enzymatic modification of $CurA_S$ peptide by CurKC and CurKC variants. $CurA_S$ (M): calcd: 2714.27 Da, obs.: 2714.34 Da; ($M\text{-}2H_2O$): calcd: 2678.23 Da, obs.: 2678.67 Da; ($M\text{-}H_2O$): calcd: 2696.25 Da, obs.: 2696.75 Da; ($M+Na$): calcd: 2737.26 Da, obs.: 2737.90 Da; ($M\text{-}2H_2O+HPO_3$): calcd: 2758.21 Da, obs.: 2758.71 Da; ($M\text{-}H_2O+HPO_3$): calcd: 2776.23 Da, obs.: 2776.82 Da; ($M+HPO_3$): calcd: 2794.25 Da, obs.: 2794.85 Da. D) Close-up view of the ATP binding site in the $CurKC_{kinase}$–ATP docking structure. ATP and interacting residues are shown as sticks, and the magnesium ions are shown as cyan spheres.

tion of the residue Ser2 (Figure S5 and S6). This result shows that $CurKC_{lyase}$ retains the function as a lyase to catalyze the phosphate elimination of a phosphorylated serine (pSer) (Figure S5). Similar results were obtained previously when using the artificially separated kinase and lyase domains of the class IV lanthipeptide synthetase VenL with its peptide substrate VenA.[5d]

To understand the mechanism of catalysis, we attempted to crystallize CurKC and its soluble variants. Only $CurKC_{kinase}$ yielded crystals of sufficient quality for diffraction. Crystal structures of $CurKC_{kinase}$ in its *apo* form and in complex with adenosine was obtained with resolution limits of 2.40 Å and 2.55 Å, respectively (Table S1, Figure S7A,B and Figure S8).[10] In both crystal structures, two identical $CurKC_{kinase}$ protomers exist in one asymmetric unit with root-mean-square deviation (RMSD) values of 0.34 Å, although $CurKC_{kinase}$ is a monomer in solution (Figure S7A–C). Structural comparison of *apo*-$CurKC_{kinase}$ and the $CurKC_{kinase}$–adenosine complex reveals that the binding of adenosine caused no significant alteration of the overall conformation of $CurKC_{kinase}$ (Figure S7D).

In the $CurKC_{kinase}$–adenosine binary complex, $CurKC_{kinase}$ adopts a typical two-lobed structure as that observed for protein kinases such as PknB and PknG from *Mycobacterium tuberculosis* (Figure 2A and Figure S9A).[11] The N-lobe (residues 218–309) comprises five β-strands and an α-helix (residues 267–282, denoted as helix C), and the C-lobe (residues 310–472) is composed of six α-helices and two β-sheets. The adenosine resides in a deep cleft formed between the two lobes.

The binding between CurKC and ATP-γ-S is saturated at an ≈1:1.2 molar ratio, as determined by isothermal titration calorimetry (ITC) analysis (Figure S10), indicating that CurKC contains a single ATP binding site. In the $CurKC_{kinase}$–adenosine complex, the adenine motif is bound to the backbone carbonyl oxygen of residue E306 and the backbone amide nitrogen of residue I308 (Figure 2B). A water molecule that coordinates to the amide oxygen of I380 forms additional hydrogen bonds to adenine N6 and N7. Double mutation of E306 and I308 to Ala resulted in CurKC E306 A/I308 A with significantly impaired its phosphorylation and dehydration activity, supporting the roles of E306 and I308 for adenine binding (Figure 2C).

To provide a comprehensive view of ATP binding by $CurKC_{kinase}$, we replaced the adenosine with ATP and complemented two Mg^{2+} ions using the tLeaP module of the AMBER 16 software package.[12] The system was equilibrated by molecular dynamics (MD) simulations (Figure S11). In the docked $CurKC_{kinase}$-ATP binary structure, the two Mg^{2+} ions were chelated by the D363/N368 and D381/E383 pairs and interacted with the β- and γ-phosphates of ATP (Figures 2D). Ala substitutions of residues D363, N368, D381, and E383 abolished the activity of CurKC (Figure 2C), confirming their roles in ATP and Mg^{2+} binding and catalysis.

Despite their structural similarity, several structural differences are observed between $CurKC_{kinase}$ and kinases PknB/PknG. The D381–F382–E383 motif in $CurKC_{kinase}$ is highly conserved among LanKC and LanL enzymes and chelates Mg^{2+} through the D381/E383 pair in the docked $CurKC_{kinase}$–ATP model (Figure 2D and S12). Both D381 and E383 are indispensable for the kinase activity of CurKC (Figure 2C). In contrast, the homologous D293-F294-G295 motif in PknB lacks a second Mg^{2+} coordinating residue (Figure S9B and S12). The loop region connecting sheets β1 and β2 (spanning residues 230–236, named Loop1, Figure 2A) in $CurKC_{kinase}$ is highly conserved among LanKC enzymes but shares no sequence similarity to its structural homologs in PknG/PknB, the P-loop (Figure S12).[13]

CurKC and $CurKC_{kinase}$ are capable of modifying $CurA_S$ but not $CurA_{S\_CP}$, indicating that both enzymes are leader-dependent (Figure S5 and S16). Indeed, CurKC binds to the CurA leader peptide ($CurA_{LP}$) and the $CurA_S$ peptide with similar K_D values of 5.5 ± 0.7 μM and 3.5 ± 0.3 μM, respectively, but showed no binding with $CurA_{S\_CP}$ (Figure 3A and Figure S17 and S18), indicating that $CurA_{LP}$ is essential for enzymatic recognition. $CurKC_{lyase\text{-}kinase}$ and $CurKC_{kinase}$ bind to $CurA_{LP}$ with K_D values of (84 ± 12) μM and (801 ± 171) μM, respectively, whereas $CurKC_{lyase}$ showed no measurable binding affinity to $CurA_{LP}$ (Figure 3A). These results indicate that the kinase domain of CurKC is responsible for leader binding. The gradually decreased binding affinities of $CurKC_{lyase\text{-}kinase}$ and $CurKC_{kinase}$ to $CurA_{LP}$ compared with CurKC might be due to the structural destabilization caused by protein truncation.

Leader peptide recognition in many RiPP biosynthetic enzymes is dependent on the so-called RiPP recognition element (RRE) motif, which typically consists of three N-terminal β-strands and a C-terminal winged helix-turn-helix motif containing a total of three alpha-helices (**Figure S19**).[3a,14] These RRE motifs usually accommodate leader peptides in the cleft between the β3-strand and α3-helix through both hydrophobic interactions and hydrogen bonding. $CurKC_{kinase}$ contains an N-terminal region spanning residues 222–309 that we named leader recognition domain (LRD), consisting of two N-terminal antiparallel β-sheets, a central α-helix, and three C-terminal antiparallel β-sheets (Figure 3B). The "3β-1α-2β" organization is distinct from typical RRE folds observed in other RiPP enzymes, and this structural unit is referred to as $LRD_{3\beta\text{-}1\alpha\text{-}2\beta}$ to highlight its structural features. To understand its function, we expressed and purified $CurKC_{LRD}$ as a fusion protein conjugated to the C-terminus of the B1 domain of streptococcal protein G (GB1). Subsequent proteolytic removal of the GB1 tag led to the production of $CurKC_{LRD}$ as a soluble protein. MST assays showed that $CurKC_{LRD}$ binds to $CurA_{LP}$ with a K_D of (1.2 ± 0.3) mM, which is comparable to $CurKC_{kinase.}$ (Figure 3A). With the LRD motif truncated, $CurKC_{kinase\text{-}\Delta LRD}$ completely lost its binding affinity to $CurA_{LP}$ (Figure S20), indicating the role of the LRD motif for peptide recognition. To further corroborate the interaction between $CurKC_{LRD}$ and $CurA_{LP}$, NMR titration experiments were carried out with ^{15}N-labeled GB1–$CurKC_{LRD}$. Chemical shift changes of the $CurKC_{LRD}$ signals in the ^{1}H-^{15}N HSQC spectra were observed when titrated with various concentrations of $CurA_{LP}$, indicating a specific interaction between $CurKC_{LRD}$ and $CurA_{LP}$ (Figure S21 and S22). Due to the limitation of protein concentration and stability, we were not able to pinpoint specific residues of $CurKC_{LRD}$ that interact with $CurA_{LP}$ by three-dimensional NMR experiments with ^{15}N and ^{13}C doubly labeled GB1–$CurKC_{LRD}$. Nevertheless, these results strongly supported the role of $CurKC_{LRD}$ as the leader recognition site.

Due to the inaccessibility to a co-crystal structure of CurKC with the $CurA_{LP}$ peptide, we performed a docking study using $CurKC_{kinase}$ and the $CurA_{(-16)\text{-}4}$ peptide to understand the substrate binding mode. As the dehydration of residue Ser2 in $CurA_S$ by CurKC was most efficient, the pentapeptide $CurA_{(-1)\text{-}4}$ extracted from the MD representative snapshot of CurA was first docked into the active site of $CurKC_{kinase}$. Then, the peptide was gradually extended at the N-terminus of CurA with residue length intervals of five amino acids to gain a starting conformation for the $CurKC_{kinase}$–ATP–$CurA_{(-16)\text{-}4}$ ternary complex (Figure 3D and Figure S23). MD simulation results showed that the binding model was most stable when the region of $CurA_{LP}$ spanning residues (−16) to (−13) was bound to $CurKC_{LRD}$ in the cleft between helix C and sheet β5 through hydrophobic interactions between residues V269/L272/L279/L282

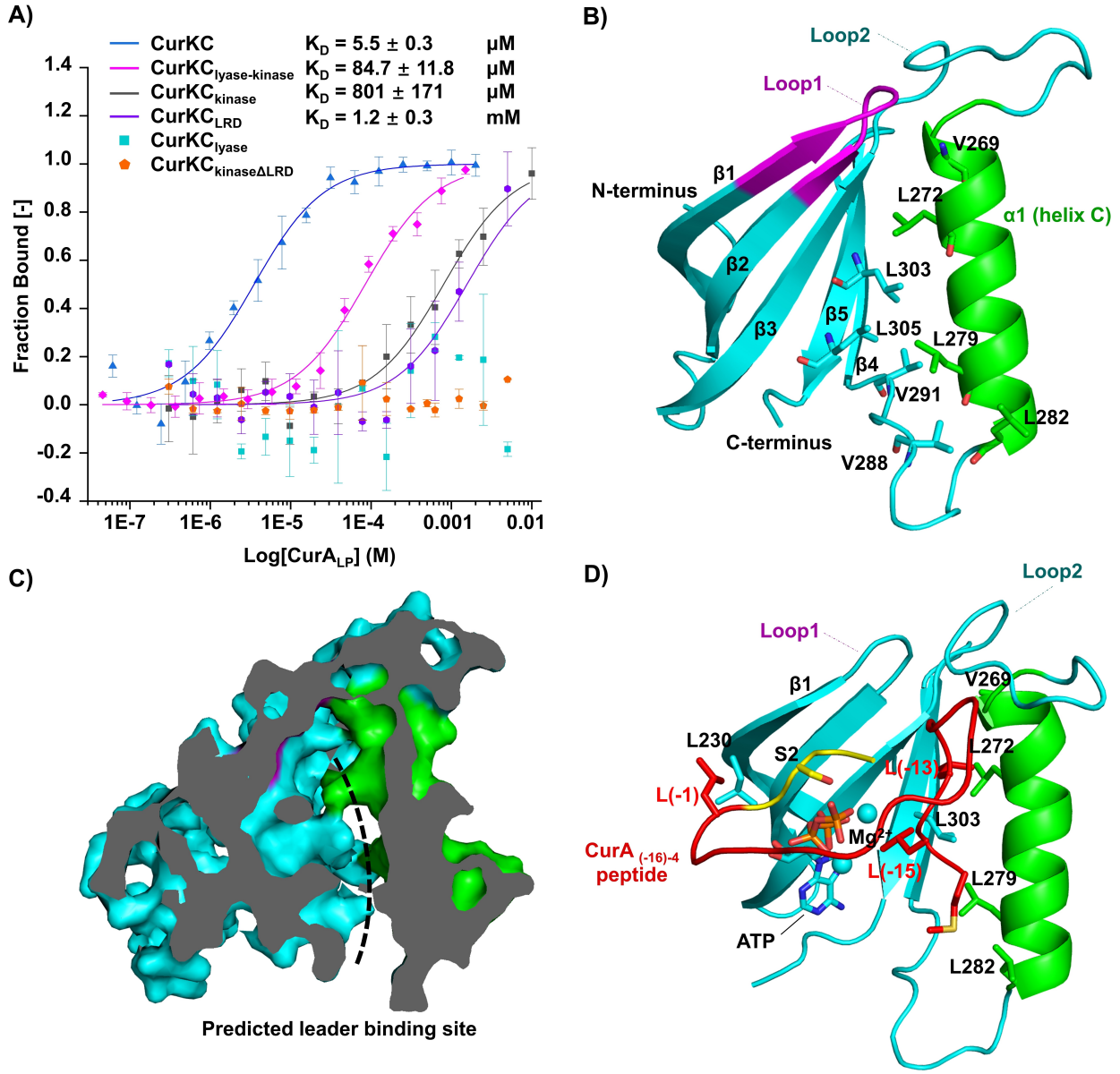

Figure 3. A) Binding affinity between the $CurA_{LP}$ peptide and the CurKC variants as measured by MST. Data represent the mean ± s.d. from three replicates. B) Structural representation of the LRD in CurKC. C) The interior view of $CurKC_{LRD}$ shows a cleft between the β1-strand and the helix C as a potential leader binding site. D) A docking model of the $CurKC_{kinase}$–ATP–$CurA_{(-16)-4}$ ternary complex. Important interacting residues are shown as sticks. The leader and core segments of peptide $CurA_{(-16)-4}$ are shown in red and yellow, respectively.

in helix C of $CurKC_{LRD}$ and residues L(−15) and L(−13) of $CurA_{LP}$ (Figure S23 and S24). Residues V269/L272/L279/L282 of CurKC are highly conserved in LanKC enzymes (Figure S25). Residues L(−15) and L(−13) of $CurA_{LP}$ are part of the proposed amphipathic "LXXLXXL" motif conserved in class III/IV leader peptides, which is important for enzymatic recognition (Figure S26).[6,9b] The "LXXLXXL" motifs in the leader peptides of several class III/V lanthipeptides display tendency to adopt an α-helical conformation.[25] However, secondary-structure prediction and circular dichroism (CD) spectroscopy analysis indicated that $CurA_{LP}$ has no tendency for α-helix formation (Figure S26), which agrees with the extended conformation of $CurA_{LP}$ in the docking model. In addition to the hydrophobic interactions, hydrogen bonding was also observed in the docking model between residues M(−16)/D(−14)/Q(−12)/M(−10) of $CurA_{LP}$ and residues K253/A263/R271/E275 of $CurKC_{LRD}$ (Figure S27).

Mutagenesis studies were then performed to evaluate the key interacting residues between $CurKC_{LRD}$ and $CurA_{LP}$ revealed in the docking model. Single and double mutations of residues V269/L272/L279/L282 all resulted in CurKC mutants with significantly impaired leader binding affinity and catalytic activities (Figure 4A, 4C and Figure S28). Similarly, mutations of K253/R271/E275 decreased the $CurKC_{LRD}$–$CurA_{LP}$ binding affinity by 20–500-fold and al-

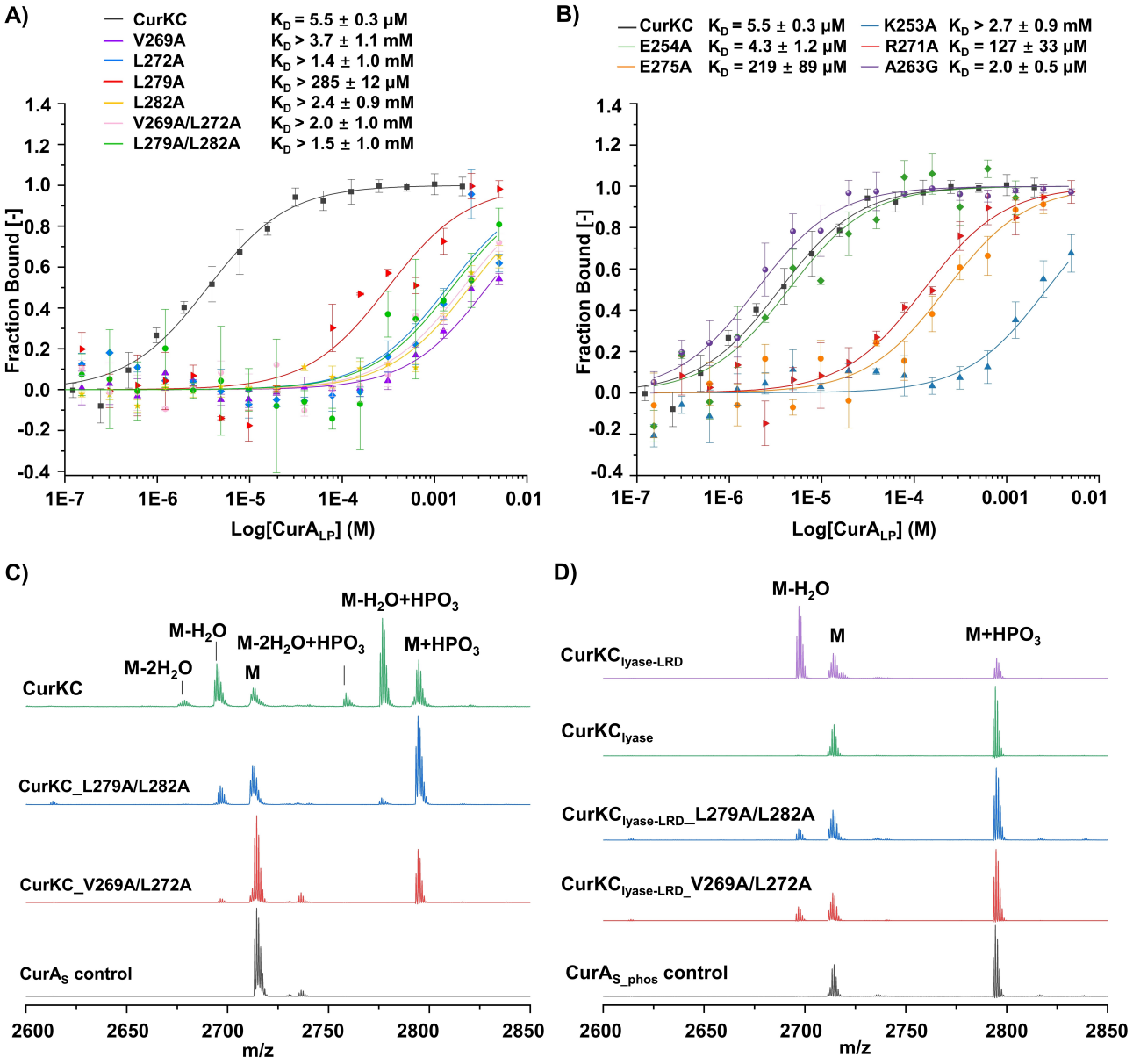

Figure 4. A,B) Binding affinities between $CurA_{LP}$ and CurKC variants as measured by MST. Assays were performed using fluorophore-labeled CurKC variants (2.5 nM) and unlabeled $CurA_{LP}$. Data represent the mean ± s.d. from three replicates. C) Modification of $CurA_S$ by CurKC and CurKC variants as determined by MALDI-TOF MS analysis. $CurA_S$ (M): calcd: 2714.27 Da, obs.: 2714.34 Da; (M–$2H_2O$): calcd: 2678.23 Da, obs.: 2678.67 Da; (M–H_2O): calcd: 2696.25 Da, obs.: 2696.75 Da; (M–$2H_2O$ + HPO_3): calcd: 2758.21 Da, obs.: 2758.71 Da; (M–H_2O + HPO_3): calcd: 2776.23 Da, obs.: 2776.82 Da; (M + HPO_3): calcd: 2794.25 Da, obs.: 2794.85 Da. D) Modification of monophosphorylated $CurA_S$ by $CurKC_{lyase}$, $CurKC_{lyase\text{-}LRD}$ or $CurKC_{lyase\text{-}LRD}$ variants. Assay composition: 20 mM Tricine (pH 8.0), 1 mM EDTA,10 µM protein, and 100 µM monophosphorylated $CurA_S$ peptide. Assay reactions were run at 25 °C for 15 h before MS analysis. $CurA_{S\text{-}phos}$ was obtained through the modification of $CurA_S$ by $CurKC_{kinase}$. $CurKC_{kinase}$ was inactivated by incubation at 95 °C, and $CurA_{s\text{-}phos}$ was purified by HPLC before assays. $CurA_S$ (M): calcd: 2714.27 Da, obs.: 2714.10 Da; (M-H_2O): calcd: 2696.25 Da, obs.: 2696.98 Da; (M + HPO_3): calcd: 2794.25 Da, obs.: 2794.98 Da.

most abolished their catalytic activities (Figure 4B and Figure S28). Residues E254 and A263 are suggested to interact with $CurA_{LP}$ through backbone amides, and their Ala mutations had little impact on the binding affinity (Figure 4B and Figure S27). In addition, residue R276 is located on the surface of helix C opposite to the leader binding cleft and has no contact with $CurA_{LP}$ in the docking model (Figure S29). Accordingly, no significant impact on the leader binding or enzymatic activity towards the peptide $CurA_S$ was observed when R276 was mutated to Ala (Figure S30). Collectively, these data support the predicted $CurKC_{LRD}$–$CurA_{LP}$ binding mode.

The LRD motif (residues 222–309) is located C-terminally to the lyase domain of CurKC (residues 1–217) in the amino acid sequence of CurKC, raising the possibility that the LRD motif might also facilitate the function of $CurKC_{lyase}$ during phosphate elimination. With monophosphorylated $CurA_S$ ($CurA_{S\text{-}phos}$) as a substrate, $CurKC_{lyase\text{-}LRD}$

(residues 1–309) efficiently eliminated the phosphate group by yielding a one-fold dehydrated product (Figure 4D). In contrast, $CurKC_{lyase}$ was unable to modify the $CurA_{S\text{-}phos}$ peptide. Furthermore, the lyase activity of $CurKC_{lyase\text{-}LRD\_V269\,A\_L272\,A}$ and $CurKC_{lyase\text{-}LRD\_L279\,A\_282\,A}$ were significantly impeded (Figure 4D), suggesting that the LRD motif is important for the enzymatic phosphate elimination.

Class III leader peptides often contain a spacer segment as a ruler to determine that Ser/Thr residues of proper positions C-terminally to the "LXXLXXL" recognition motif can be modified.[15] In the docking model of the $CurKC_{kinase}$–ATP–$CurA_{(-16)\text{-}4}$ ternary complex, a potential spacer segment spanning Gly(−11) to Asp(−2) of ≈35 Å in length showed no direct interactions with $CurKC_{kinase}$ (Figure 3D). This spacer is sufficiently long to deliver the core peptide residue Ser2 to the active site of the lyase domain (Figure S31). As a single leader anchoring site, the location of $CurKC_{LRD}$ at the interface of the kinase and lyase domains appears to be beneficial to mediate the translocation of the $CurA_{CP}$ between the two active sites for sequential Ser phosphorylation and phosphate elimination.

Although $CurKC_{lyase}$ was unable to recognize and modify the $CurA_{S\text{-}phos}$ peptide, co-incubation of $CurKC_{lyase}$ and $CurKC_{kinase}$ fully converted $CurA_{S\text{-}phos}$ to one-fold dehydrated $CurA_S$ with similar efficiency as $CurKC_{lyase\text{-}kinase}$ (Figure S5), suggesting that $CurKC_{lyase}$ and $CurKC_{kinase}$ might function cooperatively as a complex in the same manner as their covalently linked counterpart $CurKC_{lyase\text{-}kinase}$. Indeed, $CurKC_{lyase}$ binds to $CurKC_{kinase}$ with a K_D of 170 ± 28 μM, supporting that the $CurKC_{lyase}$ and $CurKC_{kinase}$ could form a complex in solution (Figure 5A).

To understand the formation of the $CurKC_{lyase}$–$CurKC_{kinase}$ complex, we performed structural prediction on $CurKC_{lyase}$, $CurKC_{kinase}$ and $CurKC_{lyase\text{-}kinase}$ by AlphaFold2 (Figure S32).[16] The predicted structure of $CurKC_{kinase}$ is highly similar to our crystal structure of $CurKC_{kinase}$ with a RMSD of only 0.91 Å. In the predicted structure of $CurKC_{lyase\text{-}kinase}$, the Loop1 and Loop2 of the LRD motif appear to be the major contributors to the $CurKC_{lyase}$–$CurKC_{kinase}$ association (Figure S33A). Indeed, $CurKC_{lyase}$ binds to $CurKC_{LRD}$ with a K_D of 139 ± 33 μM, whereas $CurKC_{kinase\_\Delta LRD}$ showed no binding affinity to $CurKC_{lyase}$ (Figure 5A and Figure S34). Mutations of residues S233/R234 in the LRD and residue N103 in $CurKC_{lyase}$, which are located at the domain interface in the predicted structure of $CurKC_{lyase\text{-}kinase}$, impaired the binding between $CurKC_{lyase}$ and $CurKC_{kinase}$ (Figure 5A), supporting the role of LRD in the domain interactions.

The characteristic $LRD_{3\beta\text{-}1\alpha\text{-}2\beta}$ motifs are found in all characterized LanKCs with a similar organization, as indicated by sequence analysis and structural prediction using AlphaFold2 (Figure S12, S25 and S35). Important hydrophobic residues for leader binding are well conserved in these $LRD_{3\beta\text{-}1\alpha\text{-}2\beta}$ motifs of LanKC enzymes, suggesting their universal function (Figure S25). To examine the role of the $LRD_{3\beta\text{-}1\alpha\text{-}2\beta}$ motifs in LanKC enzymes for lyase–kinase interdomain interaction, we selected AciKC from the biosynthesis of the class III lanthipeptide catenulipeptin as a model enzyme and expressed its lyase (residues 1–219) and kinase (220–495) domains as separate proteins, named $AciKC_{lyase}$ and $AciKC_{kinase}$, respectively. $AciKC_{lyase}$ binds to $AciKC_{kinase}$ with a K_D of 43.9 ± 10.9 μM (Figure 5B). Similar to CurKC, structural prediction indicates that Loop1 and Loop2 of $AciKC_{LRD}$ might be the major contributors to the $AciKC_{lyase}$–$AciKC_{kinase}$ interaction (Figure S36A). Mutations of residues at the $AciKC_{LRD}$–$AciKC_{lyase}$ interface, including S114, N236 and R258, resulted in decreased binding affinity (Figure 5B), supporting the role of $AciKC_{LRD}$ for interdomain interactions. Interestingly, $AciKC_{lyase}$ binds to $CurKC_{kinase}$ with a K_D of (209 ± 71) μM, and $CurKC_{lyase}$ binds to $AciKC_{kinase}$ with a K_D of (14.8 ± 8.3) μM (Figure 5C and Figure S37), indicating that the association of the lyase and kinase domains of AciKC and CurKC is interchangeable in vitro. Again, mutations in the Loop 1/2 of $CurKC_{LRD}$ impaired the $AciKC_{lyase}$–$CurKC_{kinase}$ binding (Figure S34), suggesting that the $CurKC_{LRD}$ participates in the interdomain association.

The lyase and kinase domains of class III and class IV lanthipeptide synthetases share sequence similarity.[6] $LRD_{3\beta\text{-}1\alpha\text{-}2\beta}$ motifs are also found at the interface of the lyase and kinase domains in the predicted structures of LanL enzymes (Figure S12, S25, S36 and S37B). To explore the role of the LRD motifs in LanL enzymes, VenL was selected as a model enzyme.[5d] MST assays showed that $VenL_{kinase}$ (residues 213–513) binds to $VenL_{lyase}$ (residues 1–212) with a K_D value of 32.3 ± 2.9 μM (Figure 5C). In addition, $VenL_{kinase}$ binds to $CurKC_{lyase}$ with a K_D of 24.3 ± 3.5 μM, and $VenL_{lyase}$ binds to $CurKC_{kinase}$ with a K_D of 177 ± 39 μM (Figure 5A-5 C and Figure S37). Again, mutations in the Loop 1/2 of $CurKC_{LRD}$ resulted in an approximately two-fold decrease in the $CurKC_{kinase}$–$VenL_{lyase}$ binding (Figure S37A). Collectively, these data indicate that the LRDs in class III and IV lanthipeptide synthetases play a role in the cross-class binding of class III/IV lyase and kinase domains.

Finally, we examined whether the catalytic function of the heterologous complex formed by kinase and lyase domains of distinct enzyme origins can be retained. Using $CurA_S$ as a model peptide substrate, $VenL_{kinase}$ displayed good substrate tolerance and converted $CurA_S$ to a monophosphorylated product (Figure 5D). Co-incubation of $CurKC_{lyase}$, $VenL_{kinase}$, and $CurA_S$ led to the formation of one-fold dehydrated $CurA_S$ (Figure 5D). As $CurKC_{lyase}$ is not able to process the phosphorylated peptide substrate independently, these results indicated that $CurKC_{lyase}$ binds to $VenL_{kinase}$ and therefore gained access to phosphorylated $CurA_S$ for catalysis. Thus, these results demonstrate that the complex of $CurKC_{lyase}$ and $VenL_{kinase}$ retained the catalytic function of each domain when using the $CurA_S$ peptide as substrate. The data also implies that $VenL_{LRD}$ is both able to recognize CurAs as a substrate and to shuttle the $CurA_s$ core peptide between the $VenL_{kinase}$ and $CurKC_{lyase}$ active sites.

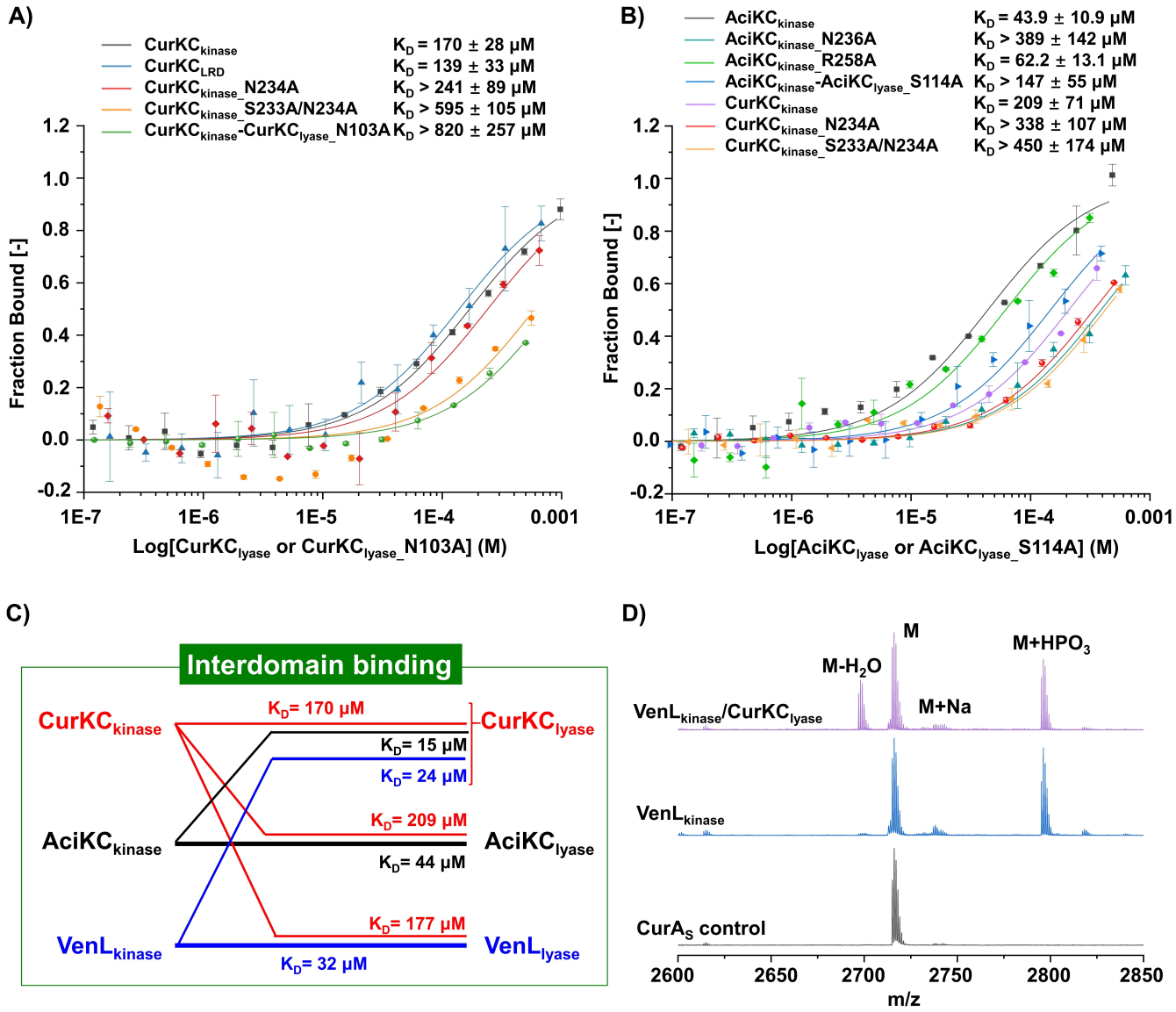

Figure 5. A) MST analysis of the binding affinities between CurKC$_{lyase}$ and CurKC$_{kinase}$ variants, as well as CurKC$_{kinas}$–CurKC$_{lyase}$ N103A. Assays were performed using fluorophore-labeled CurKC$_{lyase}$ or CurKC$_{lyase}$ N103A (2.5 nM) and unlabeled CurKC$_{kinase}$ variants. Data represent the mean ± s.d. from three replicates. B) MST analysis of the binding affinities between AciKC$_{lyase}$ and AciKC$_{kinase}$ or CurKC$_{kinase}$ variants, as well as AciKC$_{kinase}$–AciKC$_{lyase}$_S114A. Data represent the mean ± s.d. from three replicates. The binding assays were carried out using fluorophore-labeled AciKC$_{lyase}$ or AciKC$_{lyase}$_S114A (2.5 nM) and increasing amounts of unlabeled proteins. C) Interdomain binding affinities between the kinase and lyase domains of CurKC, AciKC, and VenL. D) In vitro modification of CurA$_S$ by VenL$_{kinase}$ and VenL$_{kinase}$/CurKC$_{lyase}$. CurA$_S$ (M): calcd: 2714.27 Da, obs.: 2714.93 Da; (M-H$_2$O): calcd: 2696.25 Da, obs.: 2696.96 Da; (M + Na): calcd: 2737.26 Da, obs.: 2737.13 Da; (M + HPO$_3$): calcd: 2794.25 Da, obs.: 2794.98 Da. Assay composition: 20 mM Tricine (pH 8.0), 1 mM DTT, 10 mM MgCl$_2$, 1 mM ATP, 15 µM protein, and 100 µM CurA$_S$. The reactions were quenched by the addition of MeOH after incubation at 28 °C for 15 h.

Conclusion

Class III and class IV lanthipeptide synthetases are highly modular three-domain enzymes. Although the heterologous expression of their separate cyclase domains has not yet been successful, previous studies have shown that their kinase and lyase domains can fold and function as individual proteins.[5c–f] As the first crystal structure of the kinase domain of a LanKC enzyme, CurKC$_{kinase}$ displays overall structural similarity to the protein kinases PknB/PknG. However, CurKC$_{kinase}$ shows almost no structural similarity with the class II synthetase CylM despite their common function of NTP-dependent phosphorylation of Ser/Thr residues in peptide substrates (Figure S38),[4a] suggesting that class II and class III/IV synthetases are of distinct evolutionary origins.

Leader peptide binding is crucial for all three catalysis steps of LanKC enzymes.[5c] For multidomain enzymes, the leader peptide of a substrate might anchor at a single binding site, or translocate among different binding sites to meet the requirement of each catalytic domain. In the case of the class I dehydratase NisB, the leader peptide of its

substrate NisA binds to a single LP binding site for both glutamylation and elimination.[17] The crystal structure of $CurKC_{kinase}$ reveals an unprecedented $LRD_{3\beta\text{-}1\alpha\text{-}2\beta}$ motif that plays essential roles in leader binding. Distinct from the previously discovered RRE motifs found in RiPP biosynthetic enzymes, the $LRD_{3\beta\text{-}1\alpha\text{-}2\beta}$ motifs form a hydrophobic cleft between helix C and sheet β5 for leader binding. Our docking model indicated that this cleft likely interacts with the Met/Leu residues in the **ML**D**L**QG**M** motif in $CurA_{LP}$ mainly through hydrophobic interactions. A conserved (M/L)XX(L/V)XXL motif in class III/IV leader peptides is proposed to be essential for enzymatic recognition, and alterations of the hydrophobic M/V/L residues usually impedes substrate binding and modification.[9b] Our structural analysis and mutagenesis studies were in good agreement with previous biochemical results of other LanKC enzymes. It is noteworthy that in the class IV synthetase SgbL, a ≈100 amino acid long motif ($SgbL_{208\text{-}318}$), which is equivalent to the $LRD_{3\beta\text{-}1\alpha\text{-}2\beta}$ motif of CurKC, was already identified as peptide binding site by hydrogen-deuterium exchange mass spectrometry (HDX-MS) analysis and binding assays.[5f] Similar to $CurKC_{LRD}$, the $SgbL_{208\text{-}318}$ motif is predicted to adopt a structure comprising of four antiparallel β-sheets and a central α-helix. The HDX-MS experiment strongly indicated the α-helix and sheet β4 as the major LP-binding units, which is highly similar to our model of $CurA_{LP}$–$CurKC_{LRD}$ binding. Hence, it makes sense that we also observed how enzymatic activity was retained when using domains from enzymes originating from different classes *in trans*. In contrast to the previous studies that were based on HDX-MS data and a mere prediction of the SgbL kinase domain structure, our study provides the first real three-dimensional structure of a class III kinase domain including its leader peptide binding site. This structure allowed us in turn to not only show the general function of this domain for leader binding, but also what residues in the protein form crucial contacts with the leader peptide. Furthermore, our study for the first time demonstrates the role of the $LRD_{3\beta\text{-}1\alpha\text{-}2\beta}$ motif for mediating the interactions between the catalytic centers for peptide phosphorylation and phosphate elimination, which is key for understanding how the substrate can be shuttled back and forth between active sites in a sequential manner. The binding of ATP has little impact on the leader binding and lyase–kinase association (Figure S39). This greatly expands our understanding of how the biosynthesis of both class III and IV lanthipeptides are accomplished on a molecular level.

In conclusion, our study shows that $LRD_{3\beta\text{-}1\alpha\text{-}2\beta}$ motifs are conserved among class III and class IV lanthipeptide synthetases and mediate the association between the lyase and kinase domains. The binding modes between $LRD_{3\beta\text{-}1\alpha\text{-}2\beta}$ motifs and lyase domains are highly conserved across LanKC and LanL enzymes and facilitate the binding of domains taken from distinct classes. These findings highlight the modularity and the close evolutionary relationship between the lyase–kinase domains of LanKC and LanL enzymes, despite the lack of homology among their cyclase domains.

Acknowledgements

This work is supported by the NSF of China (Grant 21922703 and 91953112 to H.W. and 31870735 to H. Y.), National Key R&D Program of China (2019YFA0905800), the Natural Science Foundation of Jiangsu Province (Grant BK20190004 and BK20202004 to H.W. and BK20200335 to W.W.). We thank the National Center for Protein Sciences Shanghai (NCPSS) beamlines BL18 U and BL19U allowance. We thank the staffs of the National Center for Protein Sciences Shanghai (NCPSS) beamlines BL18 U and BL19 U and the Shanghai Synchrotron Radiation Facility (SSRF) BL17 U, Shanghai, People's Republic of China, for assistance during data collection. We thank the High Performance Computing Center (HPCC) of Nanjing University for the numerical calculations on its blade cluster system. Open Access funding enabled and organized by Projekt DEAL.

Conflict of Interest

The authors declare no conflict of interest.

Data Availability Statement

The data that support the findings of this study are available in the supplementary material of this article.

Keywords: Biosynthesis · Domain Interactions · Lanthipeptides · Substrate Recognition

[1] a) M. Montalban-López, T. A. Scott, S. Ramesh, I. R. Rahman, A. J. van Heel, J. H. Viel, V. Bandarian, E. Dittmann, O. Genilloud, Y. Goto, M. J. Grande Burgos, C. Hill, S. Kim, J. Koehnke, J. A. Latham, A. J. Link, B. Martinez, S. K. Nair, Y. Nicolet, S. Rebuffat, H. G. Sahl, D. Sareen, E. W. Schmidt, L. Schmitt, K. Severinov, R. D. Sussmuth, A. W. Truman, H. Wang, J. K. Weng, G. P. van Wezel, Q. Zhang, J. Zhong, J. Piel, D. A. Mitchell, O. P. Kuipers, W. A. van der Donk, *Nat. Prod. Rep.* **2021**, *38*, 130–239; b) L. M. Repka, J. R. Chekan, S. K. Nair, W. A. van der Donk, *Chem. Rev.* **2017**, *117*, 5457–5520.

[2] a) F. J. Ortiz-López, D. Carretero-Molina, M. Sanchez-Hidalgo, J. Martin, I. Gonzalez, F. Roman-Hurtado, M. de la Cruz, S. Garcia-Fernandez, F. Reyes, J. P. Deisinger, A. Muller, T. Schneider, O. Genilloud, *Angew. Chem. Int. Ed.* **2020**, *59*, 12654–12658; *Angew. Chem.* **2020**, *132*, 12754–12758; b) A. M. Kloosterman, P. Cimermancic, S. S. Elsayed, C. Du, M. Hadjithomas, M. S. Donia, M. A. Fischbach, G. P. van Wezel, M. H. Medema, *PLoS Biol.* **2020**, *18*, e3001026; c) M. Xu, F. Zhang, Z. Cheng, G. Bashiri, J. Wang, J. Hong, Y. Wang, L. Xu, X. Chen, S. X. Huang, S. Lin, Z. Deng, M. Tao, *Angew. Chem. Int. Ed.* **2020**, *59*, 18029–18035; *Angew. Chem.* **2020**, *132*, 18185–18191; d) H. Saad, S. Aziz, M. Gehringer, M. Kramer, J. Straetener, A. Berscheid, H. Brotz-Oesterhelt, H. Gross, *Angew. Chem. Int. Ed.* **2021**, *60*, 16472–16479; *Angew. Chem.* **2021**, *133*, 16608–16615; e) F. Román-Hurtado, M. Sanchez-Hidalgo, J. Martin, F. J. Ortiz-Lopez, O. Genilloud, *Antibiotics* **2021**, *10*, 403–419.

[3] a) M. A. Ortega, Y. Hao, Q. Zhang, M. C. Walker, W. A. van der Donk, S. K. Nair, *Nature* **2015**, *517*, 509–512; b) B. Li, J. P. J. Yu, J. S. Brunzelle, G. N. Moll, W. A. van der Donk, S. K. Nair, *Science* **2006**, *311*, 1464–1467; c) N. Garg, L. M. A. Salazar-Ocampo, W. A. van der Donk, *Proc. Natl. Acad. Sci. USA* **2013**, *110*, 7258–7263.

[4] a) S. H. Dong, W. Tang, T. Lukk, Y. Yu, S. K. Nair, W. A. van der Donk, *eLife* **2015**, *4*, e07607; b) L. L. Xie, L. M. Miller, C. Chatterjee, O. Averin, N. L. Kelleher, W. A. van der Donk, *Science* **2004**, *303*, 679–681; c) B. Li, D. Sher, L. Kelly, Y. X. Shi, K. Huang, P. J. Knerr, I. Joewono, D. Rusch, S. W. Chisholm, W. A. van der Donk, *Proc. Natl. Acad. Sci. USA* **2010**, *107*, 10430–10435.

[5] a) W. M. Müller, T. Schmiederer, P. Ensle, R. D. Sussmuth, *Angew. Chem. Int. Ed.* **2010**, *49*, 2436–2440; *Angew. Chem.* **2010**, *122*, 2486–2490; b) N. A. Jungmann, B. Krawczyk, M. Tietzmann, P. Ensle, R. D. Sussmuth, *J. Am. Chem. Soc.* **2014**, *136*, 15222–15228; c) H. Wang, W. A. van der Donk, *ACS Chem. Biol.* **2012**, *7*, 1529–1535; d) Y. Goto, B. Li, J. Claesen, Y. Shi, M. J. Bibb, W. A. van der Donk, *PLoS Biol.* **2010**, *8*, e1000339; e) J. D. Hegemann, W. A. van der Donk, *J. Am. Chem. Soc.* **2018**, *140*, 5743–5754; f) J. D. Hegemann, L. Shi, M. L. Gross, W. A. van der Donk, *ACS Chem. Biol.* **2019**, *14*, 1583–1592; g) J. D. Hegemann, R. D. Sussmuth, *ChemBioChem* **2021**, *22*, 3169–3172; h) A. Grigoreva, J. Andreeva, D. Bikmetov, A. Rusanova, M. Serebryakova, A. H. Garcia, D. Slonova, S. K. Nair, G. Lippens, K. Severinov, S. Dubiley, *iScience* **2021**, *24*, 102480.

[6] J. D. Hegemann, R. D. Süssmuth, *RSC Chem. Biol.* **2020**, *1*, 110–127.

[7] a) K. Meindl, T. Schmiederer, K. Schneider, A. Reicke, D. Butz, S. Keller, H. Guhring, L. Vertesy, J. Wink, H. Hoffmann, M. Bronstrup, G. M. Sheldrick, R. D. Sussmuth, *Angew. Chem. Int. Ed.* **2010**, *49*, 1151–1154; *Angew. Chem.* **2010**, *122*, 1169–1173; b) G. H. Völler, J. M. Krawczyk, A. Pesic, B. Krawczyk, J. Nachtigall, R. D. Sussmuth, *ChemBioChem* **2012**, *13*, 1174–1183.

[8] B. Krawczyk, G. H. Voller, J. Voller, P. Ensle, R. D. Sussmuth, *ChemBioChem* **2012**, *13*, 2065–2071.

[9] a) S. Chen, B. Xu, E. Chen, J. Wang, J. Lu, S. Donadio, H. Ge, H. Wang, *Proc. Natl. Acad. Sci. USA* **2019**, *116*, 2533–2538; b) V. Wiebach, A. Mainz, R. Schnegotzki, M. J. Siegert, M. Hugelland, N. Pliszka, R. D. Sussmuth, *Angew. Chem. Int. Ed.* **2020**, *59*, 16777–16785; *Angew. Chem.* **2020**, *132*, 16920–16929.

[10] All crystal structures have been deposited in the PDB database under accession numbers 7WJ6 for the $CurKC_{kinase}$, 7WJ7 for the $CurKC_{kinase}$-adenosine complex.

[11] L. N. Johnson, M. E. Noble, D. J. Owen, *Cell* **1996**, *85*, 149–158.

[12] H. M. A. D. A. Case, K. Belfon, I. Y. Ben-Shalom, J. T. Berryman, S. R. Brozell, D. S. Cerutti, T. E. Cheatham, III, G. A. Cisneros, V. W. D. Cruzeiro, T. A. Darden, R. E. Duke, G. Giambasu, M. K. Gilson, H. Gohlke, A. W. Goetz, R. Harris, S. Izadi, S. A. Izmailov, K. Kasavajhala, M. C. Kaymak, E. King, A. Kovalenko, T. Kurtzman, T. S. Lee, S. LeGrand, P. Li, C. Lin, J. Liu, T. Luchko, R. Luo, M. Machado, V. Man, M. Manathunga, K. M. Merz, Y. Miao, O. Mikhailovskii, G. Monard, H. Nguyen, K. A. O'Hearn, A. Onufriev, F. Pan, S. Pantano, R. Qi, A. Rahnamoun, D. R. Roe, A. Roitberg, C. Sagui, S. Schott-Verdugo, A. Shajan, J. Shen, C. L. Simmerling, N. R. Skrynnikov, J. Smith, J. Swails, R. C. Walker, J. Wang, J. Wang, H. Wei, R. M. Wolf, X. Wu, Y. Xiong, Y. Xue, D. M. York, S. Zhao, and P. A. Kollman, *University of California, San Francisco* **2022**.

[13] a) T. A. Young, B. Delagoutte, J. A. Endrizzi, A. M. Falick, T. Alber, *Nat. Struct. Biol.* **2003**, *10*, 168–174; b) M. N. Lisa, M. Gil, G. Andre-Leroux, N. Barilone, R. Duran, R. M. Biondi, P. M. Alzari, *Structure* **2015**, *23*, 1039–1048.

[14] a) B. J. Burkhart, G. A. Hudson, K. L. Dunbar, D. A. Mitchell, *Nat. Chem. Biol.* **2015**, *11*, 564–570; b) C. A. Regni, R. F. Roush, D. J. Miller, A. Nourse, C. T. Walsh, B. A. Schulman, *EMBO J.* **2009**, *28*, 1953–1964; c) J. Koehnke, G. Mann, A. F. Bent, H. Ludewig, S. Shirran, C. Botting, T. Lebl, W. Houssen, M. Jaspars, J. H. Naismith, *Nat. Chem. Biol.* **2015**, *11*, 558–563; d) S. R. Wecksler, S. Stoll, A. T. Iavarone, E. M. Imsand, H. Tran, R. D. Britt, J. P. Klinman, *Chem. Commun.* **2010**, *46*, 7031–7033; e) T. L. Grove, P. M. Himes, S. Hwang, H. Yumerefendi, J. B. Bonanno, B. Kuhlman, S. C. Almo, A. A. Bowers, *J. Am. Chem. Soc.* **2017**, *139*, 11734–11744; f) T. Sumida, S. Dubiley, B. Wilcox, K. Severinov, S. Tagami, *ACS Chem. Biol.* **2019**, *14*, 1619–1627; g) C. Dou, Z. Long, S. Li, D. Zhou, Y. Jin, L. Zhang, X. Zhang, Y. Zheng, L. Li, X. Zhu, Z. Liu, S. He, W. Yan, L. Yang, J. Xiong, X. Fu, S. Qi, H. Ren, S. Chen, L. Dai, B. Wang, W. Cheng, *Cell Res.* **2022**, *32*, 302–314.

[15] W. M. Müller, P. Ensle, B. Krawczyk, R. D. Sussmuth, *Biochemistry* **2011**, *50*, 8362–8373.

[16] J. Jumper, R. Evans, A. Pritzel, T. Green, M. Figurnov, O. Ronneberger, K. Tunyasuvunakool, R. Bates, A. Zidek, A. Potapenko, A. Bridgland, C. Meyer, S. A. A. Kohl, A. J. Ballard, A. Cowie, B. Romera-Paredes, S. Nikolov, R. Jain, J. Adler, T. Back, S. Petersen, D. Reiman, E. Clancy, M. Zielinski, M. Steinegger, M. Pacholska, T. Berghammer, S. Bodenstein, D. Silver, O. Vinyals, A. W. Senior, K. Kavukcuoglu, P. Kohli, D. Hassabis, *Nature* **2021**, *596*, 583–589.

[17] L. M. Repka, K. J. Hetrick, S. H. Chee, W. A. van der Donk, *J. Am. Chem. Soc.* **2018**, *140*, 4200–4203.

Manuscript received: August 2, 2022
Accepted manuscript online: September 13, 2022
Version of record online: October 7, 2022